

# Development of automated workflows (spatial models) for forest monitoring with the use of time-series of multispectral optical and SAR data

Evangelos Maltezos<sup>\*a</sup>, Nikolaos Grammalidis<sup>b</sup>, Thomas Katagis<sup>c</sup>, Ioannis Z. Gitas<sup>c</sup>,  
Vasiliki (Betty) Charalampoulou<sup>a</sup>

<sup>a</sup>Geosystems Hellas S.A., Athens, Greece; <sup>b</sup>Information Technologies Institute, CERTH, Thessaloniki, Greece; <sup>c</sup>Laboratory of Forest Management and Remote Sensing, AUTH, Thessaloniki, Greece

## ABSTRACT

The significance of forest ecosystems in terms of ecosystem processes and services and impacts on humanity is fully acknowledged. The constant exploitation of natural resources and the increasing anthropogenic pressure on ecosystems continue to put a strain on and irretrievably threaten global forest ecosystems. Global forest health is declining due to climate change, air pollution and increased human activities. Protecting and monitoring the health of forest ecosystems is a vital resource management function. The technological development in the field of remote sensing provides new tools and automated solutions for forest health monitoring. An effective web-based forest health monitoring platform can contribute to ecological, social, and economic aspects. This study aims to design rapid and automated workflows (Spatial Models-SMs) for time-series forest health monitoring with flexible parameterization and user-friendly interfaces ready for feeding WPS web-GIS platforms. Those include: i) SMs that ingest available time-series data and perform pre-processing activities, ii) SMs that calculate time-series of vegetation, soil and water indices from multispectral optical imagery, iii) SMs that create colored composite images from image algebra and SAR polarizations and vi) SMs that extract change detection maps from time-series SAR data. The study area is located in the wider region of the Mouzaki, Greece, where various types of forest species can be found. Sentinel-1 & 2 data were used while the ERDAS IMAGINE software was utilized for the design of the SMs. The results indicate the potential of the designed SMs to feed WPS web-GIS platforms promptly and efficiently.

**Keywords:** Forest health monitoring, time-series, multispectral optical imagery, SAR processing, spatial models

## 1. INTRODUCTION

The constant exploitation of natural resources and the increasing anthropogenic pressure on ecosystems continue to put a strain on and irretrievably threaten global forest ecosystems. Global forest health is declining due to climate change, air pollution and increased human activities. Protecting and monitoring the health of forest ecosystems is a vital resource management function. Standard methods of assessing forest condition is through combined use of ground surveys and remote sensing means (aerial and satellite systems). Remote sensing data and methods have been extensively used for forest health studies, since they provide timely and cost-effective information at different spatial and temporal scales, thus offering insight into the dynamics of stress and mortality patterns caused by different factors<sup>1</sup>. The technological development in the field of remote sensing provides new tools and automated solutions for forest health monitoring. An effective web-based forest health monitoring platform can contribute to ecological, social, and economic aspects. Indeed, Vegetation Indices (VIs) from multispectral imagery have been broadly utilized for estimating various biophysical parameters, such as chlorophyll concentration or Leaf Area Index (LAI), which are useful for detecting and mapping stress symptoms (defoliation or discoloration)<sup>2</sup>. The broadband VIs are based on the near-infrared (NIR) and red (R) spectral bands using average spectral information over relatively broad wavelengths. That is due to the high absorption of near-infrared radiation and lower absorption of visible radiation occurring in unhealthy or stressed vegetation.

\* e.maltezos@geosystems-hellas.gr; mail@geosystems-hellas.gr, phone +30 210 2846144

Alternatively, many studies focus on the use of narrow spectral wavelengths in the visible, red-edge and NIR spectrum, since narrow-band VIs can provide more detailed information regarding the overall amount and quality of photosynthetic material (pigments: chlorophylls and carotenoids) in vegetation. Such hyperspectral information has been proven particularly useful for the development of stress-sensitive indices (e.g., normalized difference red-edge index – NDREI, perpendicular vegetation index – PRI) and assessment of the physiological status of vegetation<sup>1</sup>. Only a few hyperspectral sensors provide data with high spectral and medium to high spatial resolution (Hyperion, CHRIS/Proba)<sup>3</sup>, although recently a new generation of narrow-band multispectral satellite sensors has been designed to include off-chlorophyll absorption center wavebands (e.g. RapidEye, Worldview-2, SumbandilaSAT). Yet, image availability from the aforementioned sensors can be limited either due to distribution policies or due to high purchase costs. With the recent launch of the two Sentinel-2 sensors new opportunities arise for systematic ecosystem monitoring. The Sentinel-2 mission is providing dense series of multispectral data with 8 bands in the visible, red-edge, NIR spectrum at high spatial resolution (10-20 m, depending on the band) and at high temporal frequency (5 days at the equator).

### **1.1 Our contribution**

The need for automation to the remote sensing field prompted the development of automatic algorithms and workflows to reduce complexity and simultaneously increasing accuracy. The main objectives of such approaches are: i) the deep analysis of the contextual relations, ii) the adequate treatment of big data and data variability and iii) the presence of a critical statistical evaluation of the results obtained. Nowadays, the existence of effective tools have boosted the development of automated workflows such as Spatial Models (SMs). The SMs are automated toolkits for building, modifying, and running workflows on geospatial data<sup>4,5</sup>. This paper presents SMs for time-series forest health monitoring that exploit optical multispectral and Synthetic Aperture Radar (SAR) data. Four different types of SMs were designed: i) SMs that ingest available time-series data and perform pre-processing activities, ii) SMs that calculate time-series of vegetation, soil and water indices from multispectral optical imagery, iii) SMs that create colored composite images from image algebra and SAR polarizations and iv) SMs that extract change detection maps from time-series SAR data. The main contributions are: i) development of automated solutions ready to feed web-GIS platforms in terms of a Web Processing Service (WPS), ii) user-friendly interface (GUI) of the designed SMs, iii) flexible parameterization of the designed SMs, iv) potential high connectivity of the designed SMs through sub-SMs and v) support of a multi-modal approach, i.e., utilization and process of optical data (multispectral imagery) and SAR data.

## **2. SPECTRAL INDICES AND SAR-INTERFEROMETRIC IMAGING FOR FOREST MONITORING**

In this section, a detailed description of the calculated spectral indices from multispectral optical images and SAR-interferometric imaging associated with the forest health monitoring is carried out.

### **2.1 Spectral indices from optical multispectral imagery**

While the definition of ‘forest health’ may vary according to different social, economic and ecological perspectives, objective indicators of forest condition can be specified and measured. Forest health could be considered as a measure of a forest ecosystem's capacity to supply and allocate water, nutrients and energy so as to increase or maintain ecosystem productivity while maintaining resistance to biotic and abiotic stresses. Agents of forest health disruption, leading to forest stress, can be categorized into biotic, such as insects, fungi, bacteria, viruses, insects, parasitic plants, and abiotic, such as fires, floods and atmospheric pollution<sup>6</sup>.

Forest ecosystems are continuously influenced by abiotic and biotic agents and processes at different spatial scales (i.e. individual trees, stands, forest landscapes, entire forest types etc.) and their impact is expected to increase in frequency and severity due to climate change consequences in the coming decades<sup>7</sup>. Therefore, there is a need for the development of robust tools and methodologies that will facilitate quantitative measurements of specific indicators related to forest condition or stress at various spatiotemporal scales.

In the literature, several efficient indices have been proposed focused on the monitoring of vegetation, soil, and water. In this study, some well-known and efficient vegetation, soil and water indices were calculated as shown in Table 1. GLI, RI, VARI and NGRDI indices are helpful not only for satellite imagery, but also for aerial imagery with limited spectral information, i.e. when only RGB images are available. The GNDVI, NDVI, BRBA and NDWI exploit information from the NIR band highlighting vegetation, soil and water surfaces.

Table 1. Considered indices from optical satellite imagery

Type of index	Name of index	Equation
Vegetation	Green Leaf Index (GLI) <sup>8</sup>	$(2G-R-B)/(2G+R+B)$
Vegetation	Ratio Index (RI) <sup>9</sup>	G/B
Vegetation	Visible Atmospherically Resistant Index (VARI) <sup>9</sup>	$(G-R)/(R+G-B)$
Vegetation	Normalized Green Red Difference Index (NGRDI) <sup>10</sup>	$(G-R)/(G+R)$
Vegetation	Green Normalized Difference Vegetation Index (GNDVI) <sup>11</sup>	$(NIR-G)/(NIR+G)$
Vegetation	Normalized Difference Vegetation Index (NDVI) <sup>12</sup>	$(NIR-R)/(NIR+R)$
Soil	Band Ratio for Built-up Area (BRBA) <sup>13</sup>	G/NIR
Water	Normalized Difference Water Index (NDWI) <sup>14</sup>	$(G-NIR)/(G+NIR)$

## 2.2 SAR-interferometric imaging and polarization image algebra

The high potential of SAR data for forestry applications is known since several decades<sup>15</sup>. With the arrival of Sentinel-1, SAR based Earth Observation applications have been benefited from such this open source of dual polarization coherent data (VV and VH) with a short revisit time<sup>16</sup>. The combination of these two polarization bands offers the possibility to use the backscatter intensities from the C-Band SAR sensor for the classification of various land cover types contributing accordingly to forest health monitoring<sup>17</sup>. Each polarization includes two layers of information, that is, magnitude layer and phase (coherence) layer. Polarization image algebra based on the magnitude layer, such difference or division between the two polarizations, can also be used in order to create three-channel-color (RGB) multi-view composite images and potential feed classification algorithms (e.g. clustering methods, model-based methods, machine learning/deep learning schemes, etc.). Furthermore, interferometric products and corresponding three-channel3-color (RGB) multi-view composite images based on the phase and/or magnitude layers can contribute to the change detection task by extracting: i) coherence images, ii) interferograms, iii) Interferometric Land Use images (ILU) and vi) Multi-Temporal Coherence images (MTC). Table 2 shows the considered polarizations and image algebra as well as interferometric products from Sentinel-1 mission.

Table 2. Considered dual polarizations and image algebra & interferometric products.

Function	Colored composite images
Based on the magnitude layer for each time period	VV <sup>18</sup> (grayscale colouring)
Based on the magnitude layer for each time period	VH <sup>18</sup> (grayscale colouring)
Based on the magnitude layer and image algebra for each time period	VV, VH, VH/VV <sup>16</sup> (RGB colouring)
Based on the magnitude layer and image algebra for each time period	VV, VH, VH-VV <sup>15</sup> (RGB colouring)
Change detection for time-series data based on the phase layer	COHERENCE <sup>19</sup> (grayscale or false colouring)

Change detection for time-series data based on the phase layer

INTERFEROGRAM<sup>19</sup>  
(grayscale or false colouring)

Change detection for time-series data based on the phase and magnitude layers

ILU<sup>20</sup>  
 $R = \text{Coherence}, G = \text{Mean magnitude}, B = \text{Magnitude difference}$

Change detection for time-series data based on the phase and magnitude layers

MTC<sup>21</sup>  
 $R = \text{Magnitude layer of the first time period}, G = \text{Magnitude layer of the second time period}, B = \text{Coherence}$

### 3. APPLICATIONS

#### 3.1 Description of the area of interest

The wider area of interest is located in Mouzaki, Thessaly region, Greece (Figure 1). In Greece, 30% of the total area is covered by forests, however their contribution to the GDP is almost non-existent. An example is the chestnut production in Thessaly region of Greece, and especially in Mouzaki municipality, which is almost abandoned, due to insufficient agricultural policies concerning establishment of alternative crops, and consequently leads to loss of potential income for the rural economy. The main vegetation zones found in the Mouzaki area are: i) The Quercetion pubescentis (*Quercetalia pubescentis*) and more specifically the Quercion confertae sub-area (hilly, sub-mountainous, mountainous) and Tilio-Castanetum growth area representing mixed deciduous forests of deciduous broad-leaved forests; in this zone we have mixed forests of Oak and broadleaf broadleaf and ii) Zone of beech forests - fir and mountain coniferous conifers (*Fagetalia*) (mountainous - subalpine) and more specifically in the Fagion moosecaee sub-area and *Abietum borisii Regis* growth site, where we have forests of *Abies borisii Regis*. The main species of oak grown are *Quercus conferta*, *Q. Pubescens*, *Q. Coccifera*. Other species are the chestnut tree in the most fertile soil, the fox, the arias, the malokedros, the anchovies, the faeces, the maple, the cranium, the koutsoupia etc.

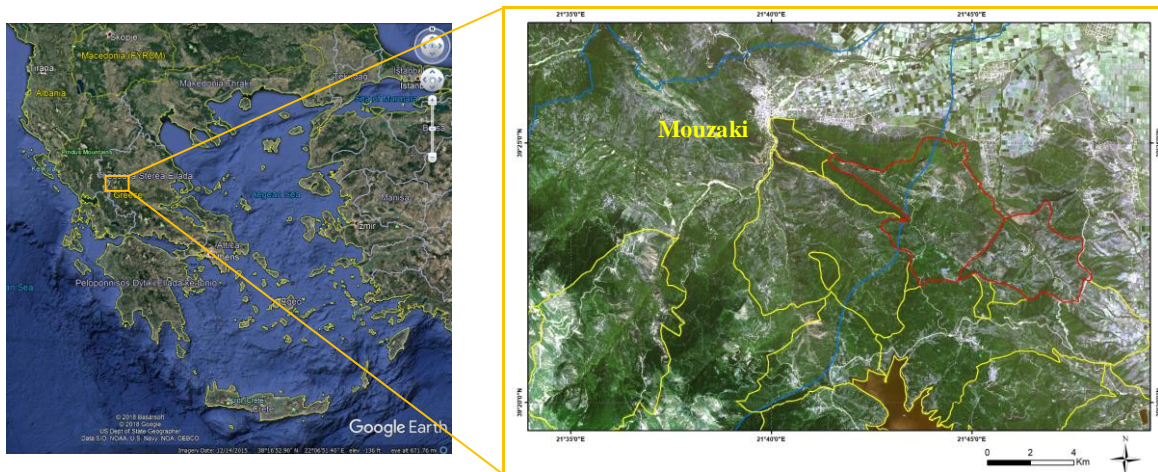


Figure 1. The wider area of interest located in Mouzaki, Thessaly region, Greece through the Google Earth Pro (in left) - ("<https://www.google.com/intl/el/earth/desktop/>").

#### 3.2 Description of the used data

In this study, data from the Copernicus/Sentinel Programme were used. In general, Copernicus is a European Union Programme aiming at developing European information services based on satellite Earth Observation data derived from Sentinel missions ("<https://www.copernicus.eu/en>"). Sentinel's data provide free use, efficient information, high temporal frequency and big area cover. More specifically, this study exploits data from Sentinel-1 & 2 missions that are freely available on ESA Scientific Data Hub website: "<https://scihub.copernicus.eu/dhus/#/home>". Table 3 shows the

main characteristics of Sentinel-1 & 2 missions and the used data of the current study. The information is compiled from the Copernicus page of the European Space Agency (ESA) website ("[http://www.esa.int/Our\\_Activities/Observing\\_the\\_Earth/Copernicus](http://www.esa.int/Our_Activities/Observing_the_Earth/Copernicus)").

Table 3. Main characteristics of Sentinel-1 & 2 missions and indication of the used data.

	Sentinel-1	Sentinel-2
<b>Launch Date:</b>	Sentinel-1A, 3 April 2014 Sentinel-1B, 25 April 2016	Sentinel-2A, 23 June 2015 Sentinel-2B, 7 March 2017
<b>Data Type:</b>	SAR data	Optical Data
<b>Instrument:</b>	C-band synthetic aperture radar (SAR) at 5.405 GHz Dual polarization coherent data (VV and VH)	Multispectral imagery covering 13 spectral bands
<b>Revisit Time:</b>	6 days	5 days from two-satellite constellation (at equator)
<b>Used data of the current study:</b>	<u>Type:</u> IW/SLC <u>Data:</u> Dual polarization coherent data (VV and VH) <u>Available information:</u> Magnitude and phase layers <u>Pixel spacing:</u> 10 m (High resolution Level-1) <u>Time period:</u> 2 August 2017, 9 August 2018	<u>Type:</u> MSIL2A <u>Data:</u> Bands: 2 (B), 3 (G), 4 (R) and 8 (NIR) <u>Pixel size:</u> 10 m <u>Time period:</u> 27 August 2017, 22 August 2018

### 3.3 Spatial models

The SMs were designed using the Spatial Modeler SDK tool via the ERDAS IMAGINE software<sup>4</sup>. The Spatial Modeler SDK tool is a C++ toolkit for building, modifying, and running workflows on geospatial data. It is extensible via a plugin mechanism where objects, such as operators, data types, and configuration dialogs, are discovered at runtime by on-demand-loading of all DLLs found in a search path and identifying the Spatial Modeler objects implemented in those DLLs are identified. The Spatial Modeler SDK can be used to build add-ons to various Hexagon Geospatial products, such as the WPS web-GIS platform of ERDAS APOLLO<sup>22</sup> and GeoMedia<sup>23</sup>. In the following, the designed SMs and the corresponding extracted results (Figures 2, 3, 4 and 5) are presented:

- *Spatial model for pre-processing activities*

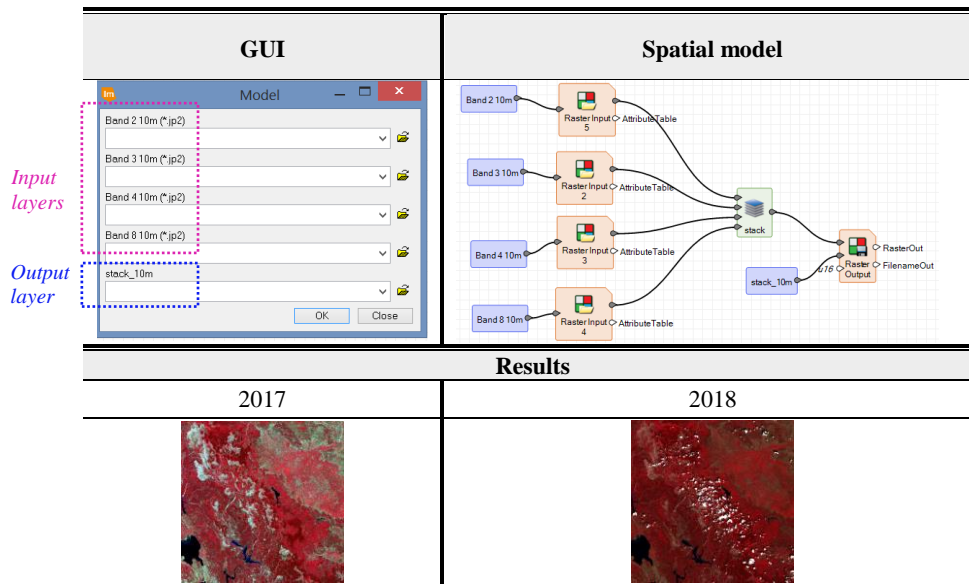


Figure 2. Spatial model and corresponding results for image stack.

More specifically, the designed SM collects, through the corresponding GUI, the individual bands of the optical satellite imagery (as input layers) and extracts the stacked image (as output layer) for each time period in terms of parallel batch processing.

- *Spatial models for vegetation, soil and water indices from optical satellite imagery*

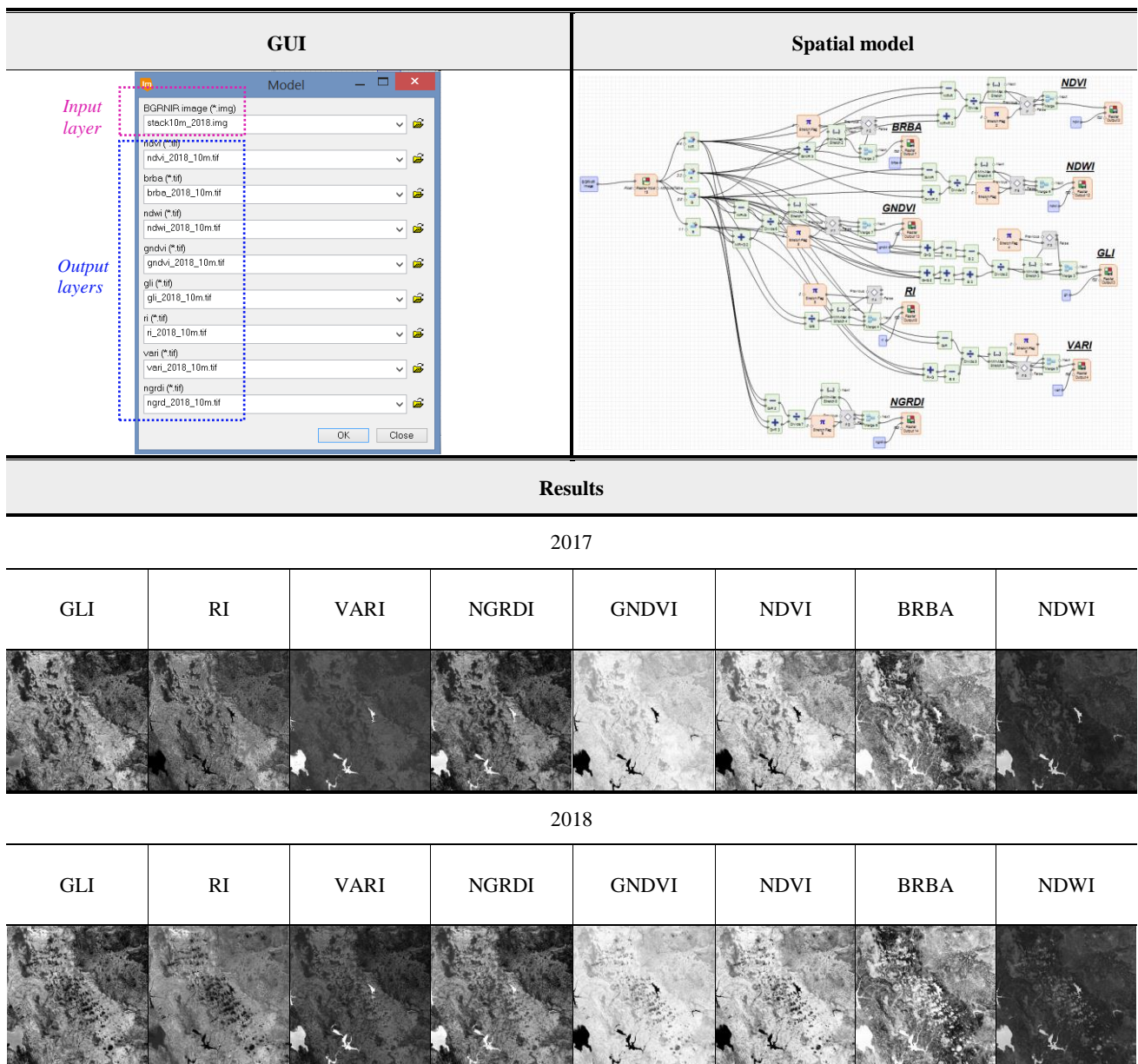


Figure 3. Spatial model and corresponding results for vegetation, soil and water indices from optical satellite imagery.

More specifically, the designed SM collects, through the corresponding GUI, the stacked image of the previous designed SM (as input layer) and extracts the considered indices of GLI, RI, VARI, NGRDI, GNDVI, NDVI, BRBA and NDWI (as output layers) for each time period in terms of parallel batch processing.

- *Spatial models for the creation of colored composite images from image algebra and SAR polarizations*

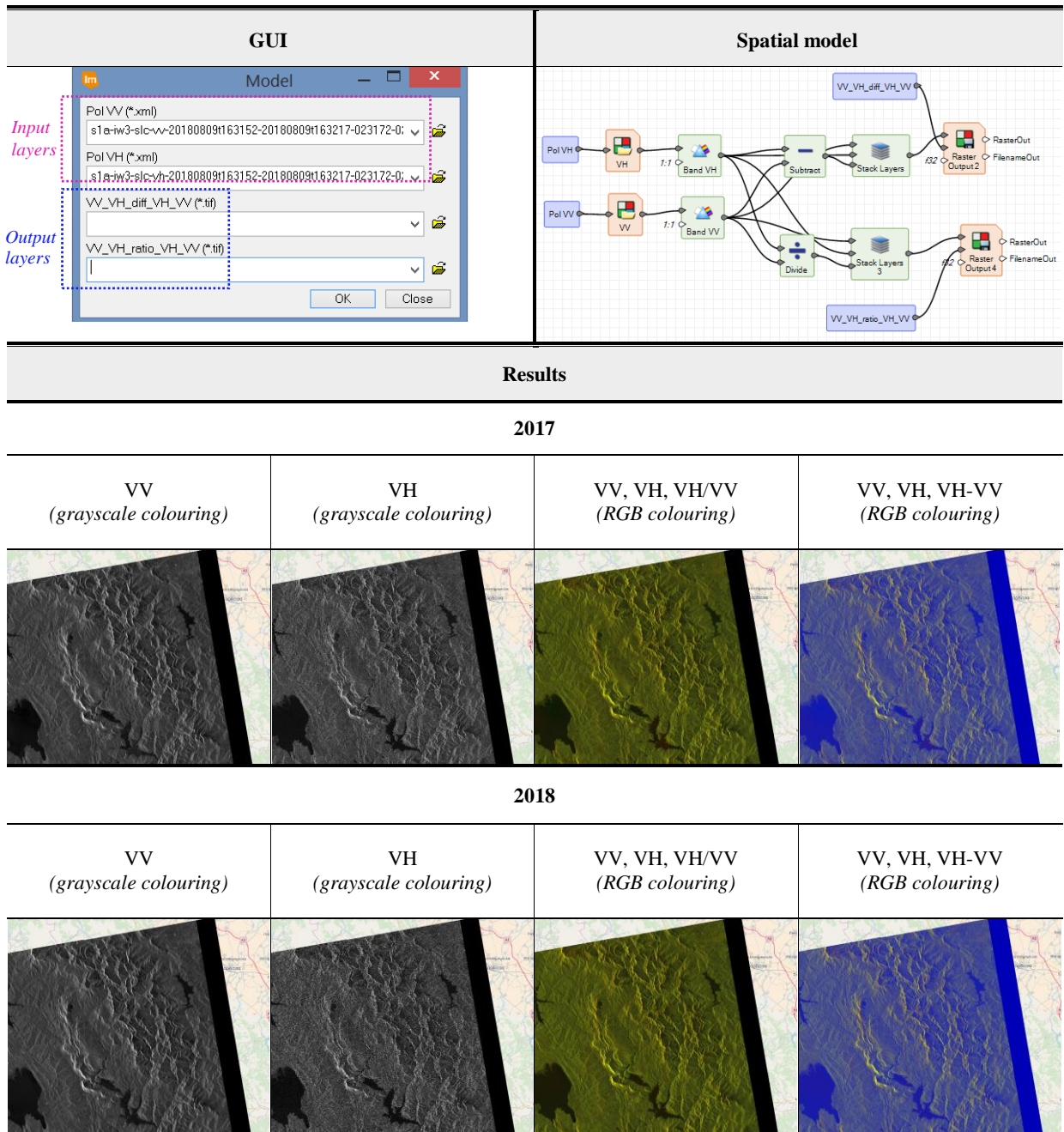
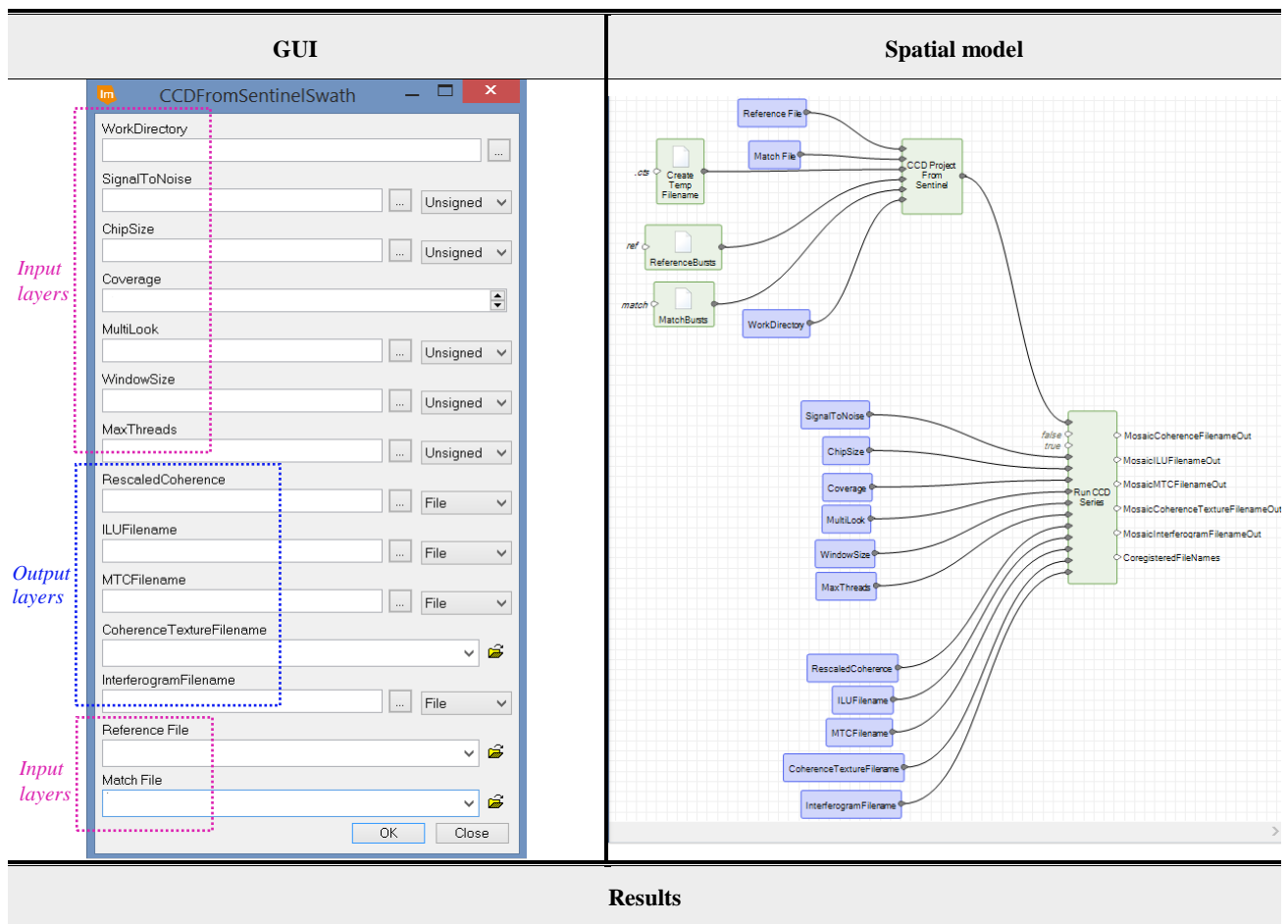


Figure 4. Spatial model and corresponding results of colored composite images from image algebra and SAR polarizations.

More specifically, the designed SM collects, through the corresponding GUI, the dual polarization coherent data of VV and VH (as input layers) and extracts the three-channel-color (RGB) multi-view composite images (as output layers) for each time period in terms of parallel batch processing.

- *Spatial models for the extraction of change detection maps from time-series SAR data*



**Change detection task between the time period of 2017-2018**

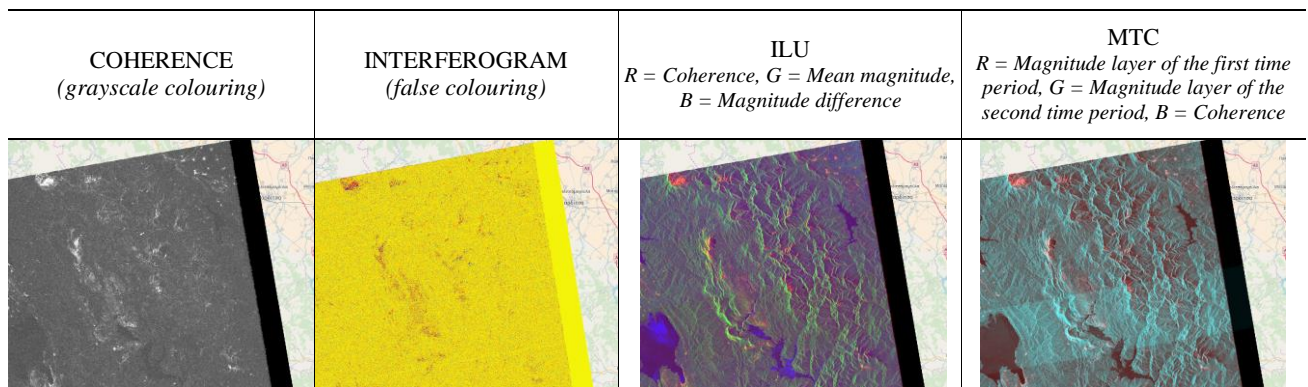


Figure 5. Spatial model and corresponding results from the change detection task using time-series SAR data.

More specifically, the designed SM collects, through the corresponding GUI, one polarization (phase layer or magnitude layer or both) of each time period (as input layers) and extracts change detection maps in terms of parallel batch processing. Also, collects the corresponding parameters and thresholds (as input layers) for the interferometry technique<sup>4,19</sup> such signal to noise, window size etc.

## 4. CONCLUSIONS AND FUTURE WORK

This paper presents automated workflows (Spatial Models-SMs) for time-series forest health monitoring using optical multispectral imagery and SAR data. Several types of SMs were designed providing automated solutions, user-friendly interface and flexible parameterization. The results indicate the ability of the designed SMs to process several types of data derived from Sentinel-1 & 2 missions in order to extract proper spectral indices and change detection maps. In addition, the results indicate the potential of the designed SMs to efficiently feed WPS web-GIS platforms. Future work is needed to design additional SMs for: i) classification tasks through machine learning schemes, ii) forest health monitoring analysis and iii) exploitation of data from other remote sensing sensors.

## ACKNOWLEDGEMENTS

This work was prepared in the framework of the ARTEMIS project, which is co-financed by the European Union and Greek national funds through the Operational Program Competitiveness, Entrepreneurship and Innovation, under the call RESEARCH – CREATE – INNOVATE (project code: T1EDK-01577).

## REFERENCES

- [1] Navarro-Cerrillo, R.M., Trujillo, J., de la Orden, M.S. and Hernández-Clemente, R., "Hyperspectral and multispectral satellite sensors for mapping chlorophyll content in a Mediterranean *Pinus sylvestris* L. plantation," *International Journal of Applied Earth Observation and Geoinformation* 26, 88-96 (2014).
- [2] Vogelmann, J.E., Xian, G., Homer, C. and Tolck B., "Monitoring gradual ecosystem change using Landsat time series analyses: Case studies in selected forest and rangeland ecosystems," *Remote Sensing of Environment* 122, 92-105 (2012).
- [3] Huang, Z. and Zhang, Y., "Remote sensing of spruce budworm defoliation using EO-1 Hyperion hyperspectral data: an example in Quebec, Canada," *Proc. of 9<sup>th</sup> Symposium of the International Society for Digital Earth* (2016).
- [4] HEXAGON GEOSPATIAL, "ERDAS IMAGINE," 2018, <<https://www.hexagongeospatial.com/products/power-portfolio/erdas-Imagine>> (5 March 2018).
- [5] HEXAGON GEOSPATIAL, "Spatial Modeler – IMAGINE," 2018, <<https://community.hexagongeospatial.com/t5/Spatial-Modeler/tkb-p/eTSpatialModeler>> (5 March 2018).
- [6] Boa, E., [An illustrated guide to the state of health of trees. Recognition and interpretation of symptoms and damage], FAO, Diagnostic and Advisory Service, CABI Bioscience, Egham, Surrey, United Kingdom, 1-46 (2003).
- [7] Niinemets, Ü., "Responses of forest trees to single and multiple environmental stresses from seedlings to mature plants: past stress history, stress interactions, tolerance and acclimation," *Forest Ecology and Management* 260(10), 1623-1639 (2010).
- [8] Booth, D.T., Cox, S.E., Meikle, T.W. and Fitzgerald, C., "The accuracy of ground-cover measurements," *Rangeland ecology & management* 59(2), 179-188 (2006).
- [9] Ok, A.O., "Robust detection of buildings from a single color aerial image," *Proc. of GEOBIA XXXVII-4/C1*, 6 (2008).
- [10] Tucker, C. J., "Red and photographic infrared linear combinations for monitoring vegetation," *Remote Sensing of Environment* 8(2), 127-150 (1979).
- [11] Moges, S.M., Raun, W.R., Mullen, R.W., Freeman, K.W., Johnson, G.V. and Solie, J.B., "Evaluation of green, red and near infrared bands for predicting winter wheat biomass, nitrogen uptake, and final grain yield," *J. Plant Nutr.* 27(8), 1431-1441 (2004).
- [12] Rouse Jr., J. W., Haas, P., Schell, J. and Deering, D., "Monitoring vegetation systems in the great plains with ERTS," *NASA Special Publication* 351, 309-317 (1973).
- [13] Kapil and Pal, P., "Comparison of Landsat 8 and Sentinel 2 data for accurate mapping of built-up area and bare soil," *Proc. of 38<sup>th</sup> Asian Conference on Remote Sensing*, 1-4 (2017).
- [14] McFeeters, S.K., "The use of the normalized difference water index (NDWI) in the delineation of open water features," *Int. J. Remote Sens.* 17(7), 1425-1432 (1996).

- [15] Dostálová, A., Hollaus, M., Milenković, M. and Wagner, W., "Forest area derivation from Sentinel-1 data," *ISPRS Annals of the Photogrammetry, Remote Sensing and Spatial Information Sciences* III-7, 227-233 (2016).
- [16] Banqué, X., Lopez-Sanchez, J.M., Monells, D., Ballester, D., Duro, J. and Koudogbo, F., "Polarimetry-based land cover classification with Sentinel-1 data," *Proc. of POLINSAR* 729, 1-5 (2015).
- [17] Balzter, H., Cole, B., Thiel, C. and Schmullius, C., "Mapping CORINE land cover from Sentinel-1A SAR and SRTM digital elevation model data using random forests," *Remote Sensing* 7, 14876-14898 (2015).
- [18] Hu, J., Ghamisi, P. and Zhu, X.X., "Feature extraction and selection of Sentinel-1 dual-pol data for global-scale local climate zone classification," *ISPRS Int. J. Geo-Inf.*, 7(379), 1-20 (2018).
- [19] Li, Z. and Bethel, J., "Image coregistration in SAR interferometry," *International Archives of the Photogrammetry, Remote Sensing and Spatial Information Sciences* XXXVII-B1, 433-438 (2008).
- [20] Schulz, K., Brunner, D. and Boldt, M., "Comparison of covamcoh and ILU image products for interferometric very high resolution SAR image pairs," *Proc. of IEEE International Geoscience and Remote Sensing Symposium*, 1-3 (2011).
- [21] Vassileva, M., Tonolo, F.G., Riccardi, P., Lecci, D., Boccardo, P. and Chiesa, G., "Satellite SAR interferometric techniques in support to emergency mapping," *European Journal of Remote Sensing*, 50(1), 464-477 (2017).
- [22] HEXAGON GEOSPATIAL, "ERDAS APOLLO," 2018,  
<<https://www.hexagongeospatial.com/products/power-portfolio/erdas-apollo>> (5 March 2018).
- [23] HEXAGON GEOSPATIAL, "GeoMedia," 2018,  
<<https://www.hexagongeospatial.com/products/power-portfolio/geomedia>> (5 March 2018).